Mechanism and Machine Theory Vol. 20. No. 3. pp. 221–231. 1985
Printed in the U.S.A.

0094-114X/85 $3.00 + .00

AN EXPERIMENTAL INVESTIGATION INTO THE DYNAMIC BEHAVIOUR OF REVOLUTE JOINTS WITH VARYING DEGREES OF CLEARANCE

R. S. HAINES
NEI Reyrolle Power Switchgear, Hebburn, Tyne & Wear, NE31 1 UP England

(*Received* 23 *April* 1984, *revised* 22 *October* 1984)

Abstract—Under static loads, the deflections associated with contact elasticity in a dry journal bearing were found to be much greater and less linear than predicted. Under a suddenly reversed uniaxial load, the air film was found to cause a dramatic change of behaviour at reduced clearances. Under a load variation representative of that at a linkage mechanism joint, the behaviour with the greatest clearance (but not that with lesser clearances) gave some support to an approximate theory published by the author.

1. INTRODUCTION

Among the causes of vibration in high-speed linkage mechanisms, clearance at the joints is likely to be particularly important, because of the greater high frequency content of impactive excitation compared with the nominal kinematic accelerations. The two-dimensional relative motions within revolute joints pose a particularly difficult problem, which has been studied by many authors in the last decade. Some details were given in a review paper[1]. References [2–10] report more recent work.† It should be understood that the joints referred to here are plain journal bearings without hydrodynamic lubrication. Since "play" rather than hydraulic effects is the dominant feature, this distinctive field of enquiry may be termed "ludodynamics".

The majority of investigations in this field have involved numerical simulations of particular mechanisms, backed up in some cases by experimental measurements that are generally shown to support the predictions. Unfortunately, in consequence of the complexity of the phenomena involved and the many variables which could conceivably affect the behaviour, it has been very difficult to reconcile the different results or to draw many general conclusions. A more fundamental empirical investigation appeared to be necessary in which the aim would be to isolate the different phenomena involved, and design tests to discriminate directly between competing models of each phenomenon rather than to seek a broad confirmation for a chosen overall model. This paper describes an experimental apparatus constructed for this purpose, and some of the results obtained. The apparatus was designed so as to minimise or exclude some of the complications normally found in a practical mechanism, so that the phenomena of primary interest could be observed more clearly. This design is described in Section 2.

One of the key problems in the study of ludodynamics at revolute joints is to predict whether the pin and journal will maintain continuous sliding contact under operating conditions, or whether episodes of contact loss and ensuing impact will occur, on the premise that the latter events are a major cause of vibration. A number of experimental investigations, for example Refs. [2, 3, 4, 16], have shown that one of the principal factors governing this aspect of behaviour is the variation of the "nominal" force vector, that is, as calculated for an ideal joint. (The actual and nominal force vectors are here denoted as **R**, **R*** respectively).

As a rule, contact loss has been found to occur near to points in the cycle when the locus of coordinates representing the components of **R*** passes close to the origin. Such points may be termed "flypasts"[1].

The experiments reported here concern three distinct aspects of ludodynamic joint behaviour, namely the elastic compliance of the contact zone under load, the dynamic reponse to a sudden reversal of a uniaxial load, and the dynamic response to a simple biaxial load variation including flypasts. The experiments are reported separately in Sections 3 to 5; their interpretation and implications are then considered collectively in the last two sections.

2. DETAILS OF APPARATUS

The mechanical arrangement of the experimental apparatus (in a typical configuration) is shown schematically in Fig. 1. The pin (*a*) of the test bearing is clamped in position, but the journal (*b*) can translate (within the "clearance circle") with 2 degrees of freedom in the vertical plane, due to the no-clearance pivots (*c*). The latter were constructed using modular flexural pivots for some tests, and

† The method used in [5, 6] has been disputed by the writer[7].

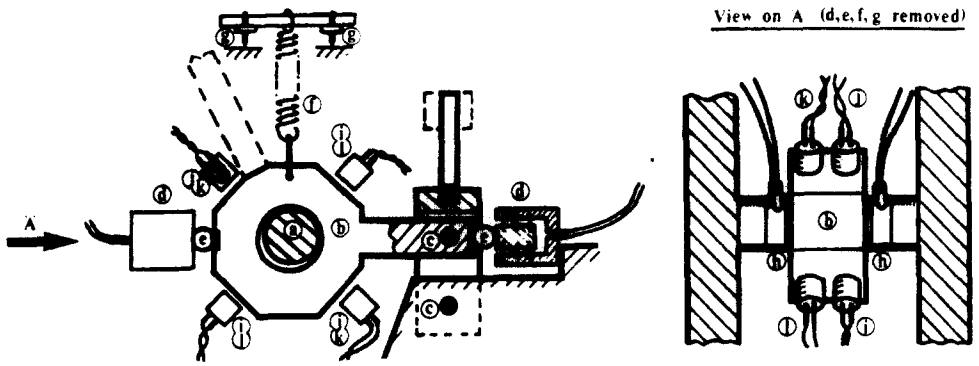

Fig. 1. Arrangement of test rig (schematic). See text for key.

instrument class ball-bearings for others. The lower no-clearance pivot is located in a "pivot stand" which is attached to the base-plate by means of two clamping screws through oversized holes and two levelling screws on a cross bar; this permits adjustment of the journal axis relative to that of the pin in two planes.

The clearance at the test bearing can be altered by exchanging the pin and/or the journal. The results reported below relate to a ground mild steel journal and three turned aluminium alloy pins denoted as *A*, *B* and *C* in order of decreasing clearance. The inertia of the links can be changed by adding masses where shown by the broken lines in Fig. 1. The leading design parameters and measured properties are listed in Table 1.

The time-varying zero-clearance joint force vector $\mathbf{R}^*$, which in a true mechanism arises in part from the inertial loading of the links as they undergo kinematic gross motion, is generated in this apparatus by a combination of pneumatic excitation, spring loading and gravity.

The purpose-built pneumatic exciter units, as shown at (*d*), act via the loading balls (*e*) and hardened pads. The pistons in these units are suspended clear of the sidewalls by two spider springs and sealing is effected by "rolling" diaphragm seals, so that Coulomb friction is entirely eliminated. Each exciter is connected by small-bore pipework to an associated master cylinder (adapted from an automobile hydraulic brake cylinder), the two systems being charged with nitrogen at a chosen pressure.

Table 1. Major parameters of apparatus

Vertical link	50 mm between joint axes; .015 kg-m^2 inertia about lower joint (standard build).
Horizontal link	125 mm between joint axes; .051 kg-m^2 inertia about no-clearance joint (standard build); 4 kg mass; 110 mm from no-clearance joint to centre-of-mass.
Bearing	50 mm nominal diameter; 27 mm (land) + 8 mm (central groove) + 27 mm (land) length; 250 μm diametral clearance with Pin A; 65 μm diametral clearance with Pin B; 20 μm diametral clearance with Pin C; 5 kHz natural frequency of supported pin alone; 1 kHz natural frequency of supported pin plus journal.
Suspension spring	780 N/mm stiffness.
Exciter system	20 mm diameter x 12 mm stroke master pistons; 20 mm diameter slave pistons; 570 N peak-to-peak load generated at 1 Hz, for 27 bar N_2; 660 N peak-to-peak load generated at 11 Hz, for 27 bar N_2; 35 bar maximum nitrogen pressure; 36 N/mm spider spring stiffness per slave piston (mean over 250 μm stroke); 16 mm loading ball diameter.
Displacement transducers	1500Ω resistive + 700Ω reactive impedance as installed; 10 V peak-to-peak driving signal at 28·5 kHz.
Load transducers	Kistler type 9063.

The master cylinder pistons are mounted on either side of an eccentric roller with a variable-speed motor drive. Thus, in the configuration shown, the net effect of the exciters is to apply to the horizontal link an alternating horizontal force of approximately sinusoidal form, with frequency equal to the eccentric shaft speed and amplitude governed by the charging pressure.

The transducers are also shown in Fig. 1. The pin load is measured by a pair of piezo-electric biaxial shear load washers (*h*), the two charge signals for each axis being added before amplification. By the use of a screw-jack and lever assembly located beneath the bearing, the journal can be poised out of contact with the pin, so that the load transducers can be zeroed. These transducers were calibrated by resting laboratory weights centrally on the journal housing.

The journal displacement along two oblique axes is measured by means of four pairs of inductances (*i* to *l*), each opposed pair forming the active arms of an a.c. bridge circuit, as shown in Fig. 2. In order to achieve an optimum specification, the inductances were hand-constructed for the purpose, each comprising copper wire wound on a ferroxide core, set in epoxy resin and cased in a short length of pipe; this was clamped, with axial adjustment, in a mounting bracket. At the driving frequency the hysteresis losses in the moving member (cast iron journal housing) are such that the resistance of the transducer is greater than the reactance, and varies more rapidly than the latter. As a consequence, both the bridge balancing elements (shown in Fig. 2) must be suitably adjusted so that the bridge output signal varies without change of phase or sign as the journal is moved across the clearance circle. The complete system was found to give satisfactory performance with signals up to 3 kHz[8]. By comparison of the demodulated and filtered displacement signals δ_i and δ_j from one measuring plane with those (δ_l, δ_k) from the other plane, alignment of the bearing can be checked to a very high accuracy, both while setting up the assembly and under dynamic conditions. This is considered to be an important advance on the previous investigations referred to, none of which appears to have incorporated such a feature. Appendix 1 outlines the alignment procedure. The jack and lever device may be used to lift the journal by a controlled amount for calibration of these transducers.

Through extensive performance tests, two potentially significant limitations of the apparatus were identified, and should be noted[8]. Firstly, the quality of the bearing surfaces was found to deteriorate rapidly. In practice, however, this did not appear to affect the repeatability of the quantitative results. Secondly, the oscillatory applied force variation was found to be materially modified by the stiffness of the spider springs in the exciter units. Under flypast conditions, this would be expected to inhibit loss of contact somewhat, the effect being greatest with high clearances and low minimum values of $|\mathbf{R}^*|$.

3. ELASTIC COMPLIANCE TESTS

The deflection of the test bearing journal under an external compressive load can be regarded as the sum of δ_s, the deflection of the pin and its supports, and δ_c, the deflection of the journal relative to the pin due to elastic deformation around the contact zone. It is the latter that is of theoretical interest here. A theoretical prediction of the load/deflection relationship may be made by adapting the standard "Hertzian" analysis for contact between cylindrical surfaces of quasi-infinite length[11], or from Dubowsky's analysis, which apparently relates to short cylindrical surfaces[12]. For a bearing of length L and radial clearance e, made of materials with Poisson's ratios ν_1, ν_2 and Young's moduli E_1, E_2, under load R, both predictions can be conveniently expressed by this formula:

$$\delta_c = Q(1 + \log_e(4e/Q) - 2\log_e(A)) \qquad (1)$$

where

$$Q = (R/\pi L)((1 - \nu_1^2)/E_1 + (1 - \nu_2^2)/E_2).$$

The term (A) has the value (2.37) for a "long" bearing and (D/L) for a "short" bearing, where D is the pin diameter. For the test bearing with pin B, the

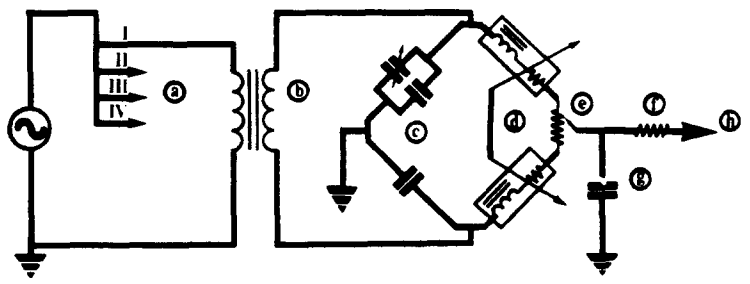

Fig. 2. Customised inductance-type displacement transducer circuit. Key: (a) channels II to IV similar to I; (b) 1:1 DC decoupler; (c) passive arms of bridge with reactive balancer; (d) push-pull pair of transducers; (e) resistive balancer; (f) 47 kΩ load to mask bridge output impedance variation; (g) 10 pF waveform distortion corrector; (h) to customised pre-amplifier, demodulator and two-stage active filter.

load/deflection relationships according to these two theories are as shown by the chain lines in Fig. 3.

Both theories referred to above assume the contact zone to be narrow relative to the pin diameter. More accurate analyses without such a restriction have been carried out numerically for particular cases[13, 14, 15], and on this basis slightly smaller predicted deflections have been reported. The author has been unable to locate any direct experimental test of the load-deflection relationship in the case of highly conformal surfaces.

The pin/support deflection δ_s was determined first. For this purpose, the bearing was assembled with thin steel plates inserted between pin *B* and the load transducer on each side. These two plates formed the uprights of a "bridge" which was completed by resting a third plate across them. A single pneumatic exciter unit and loading ball were mounted above the bearing, in a vertical attitude, so as to press down on the bridge and thus to apply load directly to the pin, the journal resting in contact with the pin under its own weight alone. Thus the journal deflection may be taken to be δ_s. With the exciter pressure varying cyclicly, the load and the journal displacement were simultaneously recorded on a digital storage oscilloscope (using summed DC signals from the two load and four displacement transducers, respectively), and then played back to an *X-Y* pen plotter. The result is shown by the broken line in Fig. 3.

The top plate of the bridge was then removed, and the exciter lowered to apply load to the journal housing, which at this stage was disconnected from the remainder of the horizontal link. The load deflection relationship was recorded as before and is shown by the solid line in Fig. 3. Despite the high amplification of the displacement signal, the noise level was negligible: the trace was repeatable: and results with a cyclic load variation at about 11 Hz and at about 0.017 Hz were virtually indistinguishable.

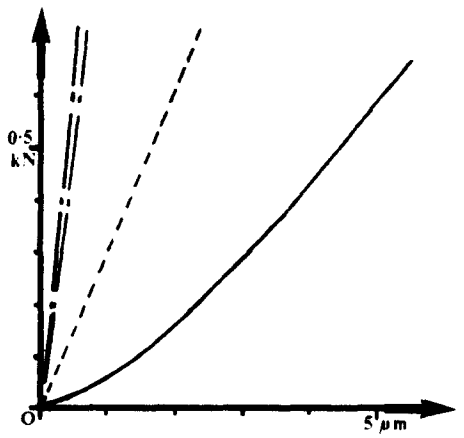

Fig. 3. Static load-deflection relationships. Key: (–·–·–) theoretical deflection for "long" and "short" bearings: (——) measured total deflection: (– – – –) measured deflection of pin supports alone.

The difference in the δ direction between the full line and the broken line is assumed to represent the surface compliance (δ_c). It is seen to be much greater than predicted, and the relationship is far less linear than predicted.

4. DROP TESTS

The purpose of the tests reported in this section was to determine the dynamic loads on the pin and the motion of the journal when the latter is allowed to drop across the clearance, from the top to the bottom contact position. The expected behaviour according to almost all the theoretical models reviewed in Ref. [1] would be an alternation between two distinct phases, sometimes termed "free-flight" and "impact" phases. During a free-flight phase, the load on the pin would be zero and the displacement of the journal axis would show a constant acceleration downwards, of about 10.6 m/sec^2 for the test linkage. (The quantitative calculations are outlined in Appendix 2.) During the impact phase, both the load and displacement curves would approximate to half-sine waves with a duration of about 0.37×10^{-3} sec, the peak load being about $2.8 \times 10^4 V$, where V is the root mean square of the impact and recoil velocities, and SI units are used throughout. These predictions only apply, however, if the impact peak load is large relative to the gravitational load. The theories differ in regard to the relationship between the approach and recoil velocities.

To test these predictions, the pneumatic exciters were removed, and the spring shown at (*f*) in Fig. 1 was replaced by a light hook suspended from a light cross-beam resting on two moveable supports. The positions of these were adjusted by hand until the transducers showed the journal just to be touching the pin at the top of the clearance circle, and the vertical link was fixed. One of the cross-beam supports was then jerked away, the resulting variation in vertical load and displacement being recorded at high speed on the digital storage oscilloscope and then played back at a low speed to the *X-Y* pen plotter. This test was performed with each pin (*A*, *B*, *C*) in turn installed in the bearing. In the case of pin *A*, a minimal trace of oil had been applied to the pin, whereas in the other cases both joint members had been degreased.

Tracings of the recorded pen plots are shown in Fig. 4. (The different vertical scales should be noted.) Those for pins *A* and *B* showed excellent repeatability, but those for *C* varied, so three different records are shown for comparison.

With the largest clearance (pin *A*) the recorded behaviour is seen qualitatively to conform to the theoretical expectations very well, the minor exceptions being an adhesive force at the outset (evidently due to the oil film), a rounded start to the load pulses, and a 5 kHz oscillatory load (free vibration of the pin) at point *a*. Quantitatively, the

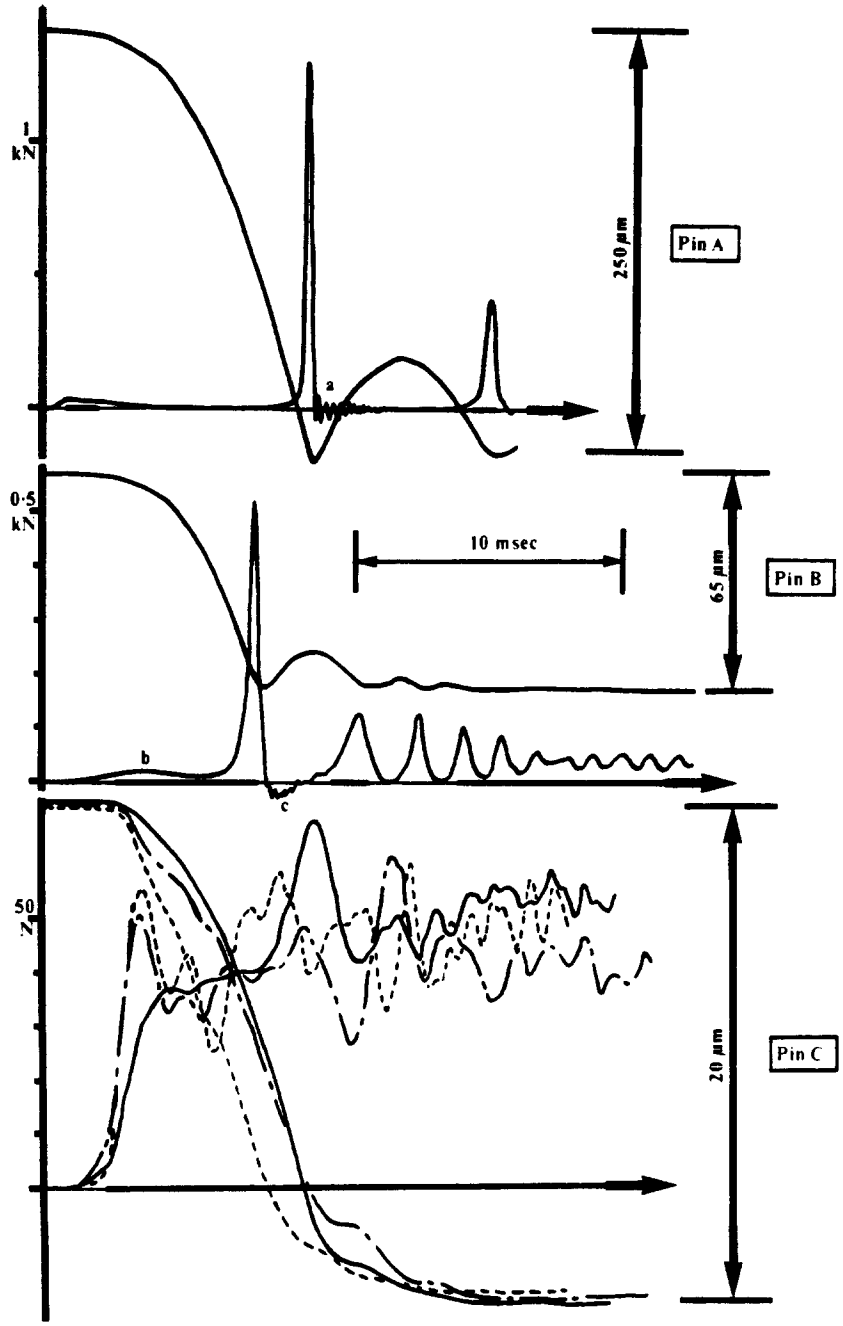

Fig. 4. Records of load on pin and displacement of journal versus time in drop tests. (——, – – –, –·–): three consecutive records.

measured acceleration and the peak force/V ratio are each about 15% smaller than predicted, while the period of the "pulses" seems rather larger, but these differences are within the margin of experimental error that might be expected.

However, the reduction of clearance is seen to bring about a dramatic change of behaviour, and contradiction of the theoretical model. Already with pin B, a significant proportion of the weight of the journal is felt by the pin while the former is in free-flight (at point b), and the acceleration is correspondingly reduced to about 6 m/sec^2. As the journal bounces upwards, moreover, it is seen to impart a "sucking" force to the pin at point c. With pin C in place the journal accelerates at no more than 1 m/sec^2. After the first two milliseconds, although the journal is still in mid-clearance, most of its weight is transmitted to the pin. Rebounds are seen to be entirely eliminated in this case. It seems clear that, at these small clearances, the theoretically disregarded effects of the air film in fact have a dominant influence, although the details of the phenomenon are evidently complex. The non-repeatable oscillations in the load trace suggest an unstable and non-linear interaction between the motion of the journal and that of the air film. There

is a clear need for a more thorough investigation into such behaviour than was possible in the context of this investigation.

5. FLYPAST TESTS

The response of the test bearing to load variations including flypasts was studied by applying a small, approximately constant force to the journal on one axis, and a relatively large, cyclicly alternating force on the other. Flypasts then occur twice per cycle as the latter component changes sign; they may be characterised quantitatively by the magnitude of the first component ($|R_V^*|$) and of the rate of change of the second ($|\dot{R}_H^*|$) at the instant concerned. For the tests reported here, R_H^* is the horizontal component and R_V^* the vertical component. According to the "empirical criterion" of Earles and Wu[16], contact is expected to be lost for such a load variation if ($|\dot{R}_H^*| / R_V^{*2}$) > 1 (N^{-1} sec^{-1}), irrespective of the radial clearance (e) or the mass distribution. According to the standard flypast theory of Haines[8,17], a flypast gives rise to a series of minima in ($|\mathbf{R}|$), any of which may permit contact loss. The first minimum is associated with the passage of the contact point from one side of the bearing to the other—the "passage" phase—and the remainder with subsequent oscillations of the contact point about the direction of $\mathbf{R}^*$—the "terminal" phase. The theory predicts that, for the load variation described, contact loss will occur in the passage phase if ($|\dot{R}_H^*|/\sqrt{|R_V^*|^3}$) > $B_p/\sqrt{e}$ and in the terminal phase if ($|\dot{R}_H^*|/\sqrt{|R_V^*|^3}$) > $B_t/\sqrt{e}$ where B_p and B_t are functions of the mass distribution. In this report, attention will be concentrated on the passage phase, and all results will be for a particular mass distribution taken as "standard".† The corresponding value of B_p was calculated to be 5.5 kg (see Appendix 2 for calculations). The term ($|\dot{R}_H^*|/\sqrt{|R_V^*|^3}$) may be regarded as an index of flypast severity. Its value at the onset of contact loss will be denoted by Q.

The experimental apparatus was set up for these tests in the configuration shown in Fig. 1, so that R_H^* is the resultant force from the two pneumatic exciters d (+ from left to right), and R_V^* the resultant of the weight of the horizontal link effective at the bearing and the force due to the soft spring f (+ downwards). With the links and exciters accurately aligned, the spring tension was adjusted until the measured static vertical load on the pin (R_V^* was a chosen value—4N or 8N. The mid-stroke gas pressure in the exciters was set to an appropriate level, and the eccentric system was set in motion. Signals from the four displacement transducers were displayed on two oscilloscopes so that the measured motion at the back and front of the bearing could be compared. Final adjustments were than made to the alignment of the links so as to minimise the discrepancy between these loci.

One pair of orthogonal displacement signals (δ_i, δ_j), together with the orthogonal pin load signals (R_H, R_V) were recorded on a four-track frequency-modulated tape-recorder with a tape-speed of 15 inches/second, while the exciter drive motor speed was varied from minimum to maximum and back again. This was repeated with each of the three pins (A, B, C) installed in the bearing in turn. The recordings were subsequently played back at 1.5 inches per second and studied with the aid of storage oscilloscopes and a pen plotter.

Similar tests were performed without the tape-recorder, with different values of R_V^*. In each case an estimate was made of the value of $|\dot{R}_H^*|$ when contact loss just occurs. Appendix 3 describes how this estimate was made.

Results were taken both with a minimal trace of oil on the bearing surfaces and after degreasing them.

Figures 5, 6 and 7 for pins A, B and C respectively show the development of the load and displacement vector loci as $|\dot{R}_H^*|$ increases. The displacement loci are for a full cycle, and the load loci for a half-cycle (one flypast). (In Fig. 5 both half-cycles of the load locus are shown, but are separated for clarity.) S and T indicate simultaneous points on the two traces so marked, determined from synchronised traces of the four recorded signals against time.

The results for pin A have been analysed in some detail elsewhere[18]. More briefly—contact loss in

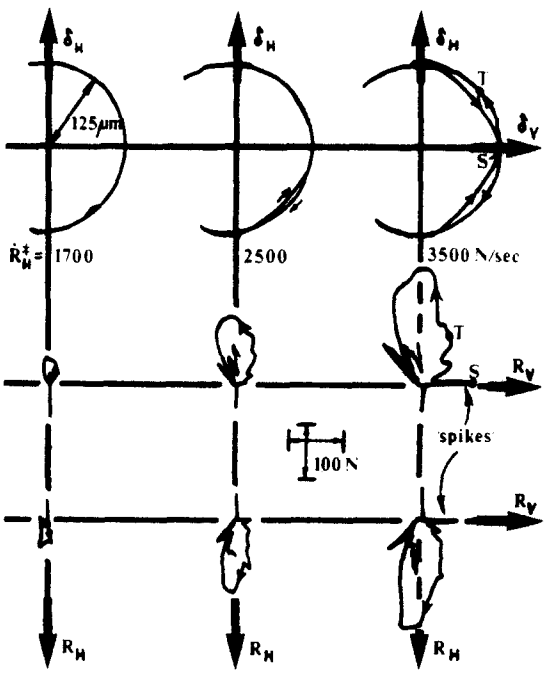

Fig. 5. Loci of journal displacement and of pin load vector during accelerating sequence of flypasts, using Pin A.

† Tests with other mass distributions were also performed[8, 18]. Results for the terminal phase were inconsistent with the standard flypast theory, apparently because of the major influence of elastic effects in this phase.

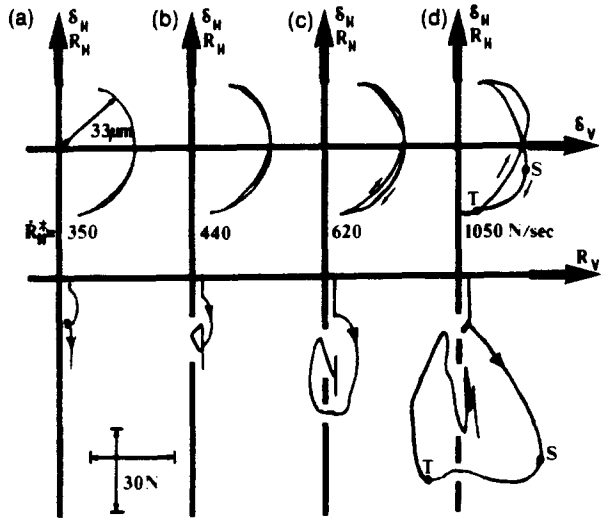

Fig. 6. Loci of journal displacement and of pin load vector during accelerating sequence of flypasts, using Pin *B*.

one direction can just be observed in the displacement locus for $\dot{R}_H^* = 2500$ N/sec, and is clearly apparent in both directions for $\dot{R}_H^* = 3500$ N/sec. The load vector locus includes an impact "spike" in the $+R_V$ direction in the cases where contact loss has occurred, followed by a "loop" associated with the acceleration and deceleration of the journal as it slides around the clearance circle. The deceleration is particularly abrupt and gives rise to a series of vibrations, probably with marginal (terminal) contact loss at one point.

With the tighter pins the behaviour is seen to be markedly different. In neither Fig. 6d nor Fig. 7b is there a trace of a load spike at the time of impact: indeed, the transition between the free-flight and contact phases is undetectable in the force locus since force is transmitted throughout. For example at point *S* in Fig. 7b a force of 35 N is transmitted through the air film, much as in the "drop tests" described earlier.

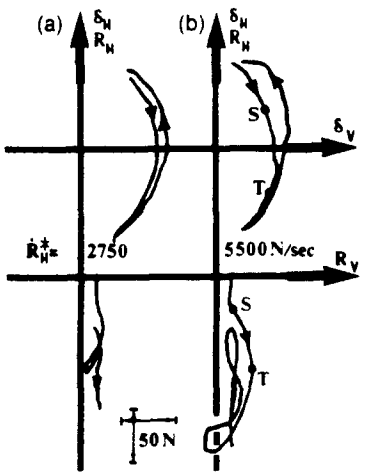

Fig. 7. Loci of journal displacement and of pin load vector during accelerating sequence of flypasts, using Pin *C*.

The visible discrepancy between the displacement loci in the forward and reverse directions in curves (a) of Figs. 6 and 7 was still present even under quasi-static conditions (that is with $\dot{R}_H^*$ slowly changed by hand pressure), so it cannot be evidence of contact loss. In fact, using pin *C* the displacement loci in both directions varied gradually but continuously as $|\dot{R}_H^*|$ was increased from zero. True contact loss was considered to have occurred, however, only when the locus began to develop relatively straight portions which extended fairly rapidly (see curves 6c and 6d).

Estimated values of $\dot{R}_H^*$ at which contact loss begins to occur were used to construct Figs. 8 and 9, for lightly oiled and degreased bearing surfaces, respectively. The values for pin *C* are necessarily very approximate in view of the behaviour just mentioned. Appendix 4 describes the basis for these figures more fully. The values are expressed as the flypast severity term Q, that is $|\dot{R}_H^*| / |R_V^*|^3$, for easy comparison with the relationship predicted by the standard flypast theory, shown by a double line.

The corresponding values of the term $(|\dot{R}_H^*| / |R_V^*|^2)$ are all in the range 110 to 1100, with a logarithmic mean of 500 ($N^{-1}sec^{-1}$), which is to be compared with the value of 1 (N^{-1} sec^{-1}) suggested by the "empirical criterion" of Earles and Wu[16].

It is seen that the order of magnitude of the transitional contact loss values for the slack pin *A* with lightly oiled surfaces agrees with that predicted, with a bias on the low side that is significantly increased when the surfaces are degreased. When the clearance is reduced, however, the transition values do not increase as predicted, but rather to the contrary.

The insensitivity of the contact loss transition to the clearance is consistent with the empirical criterion, but the order of magnitude of the latter is seen to be quite inapplicable in this case.

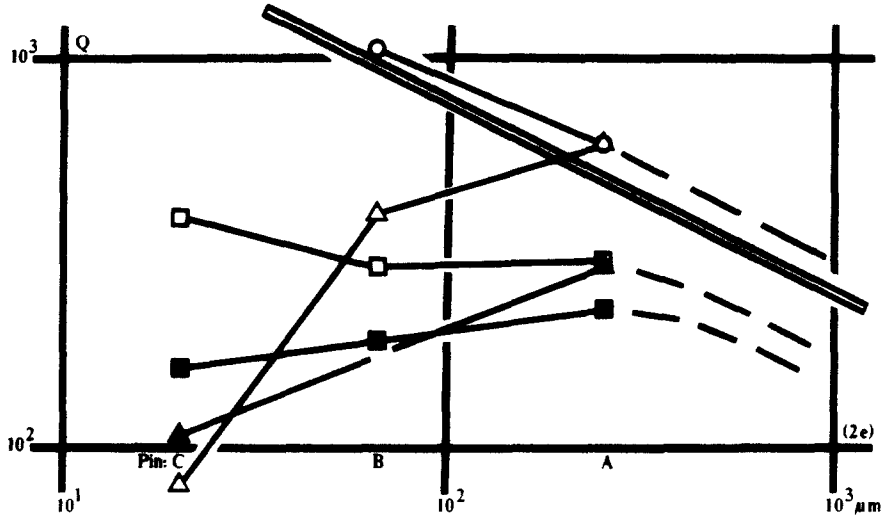

Fig. 8. Flypast severity term Q at onset of contact loss versus diametral clearance $2e$ for minimally oiled bearing. Key: $Q \equiv (|R_H^*|/|R_1^*|^{3/2})$ in units of (N/sec)/($N^{3/2}$): (═══) theoretical variation of Q. (○ △ □ ▲ ■) Measured values of Q | R_1^* | in the following ranges: (○) 0.9–1.6 N: (△) 1.6–2.8 N: (□) 2.8–4.8 N: (▲) 4.8–9N: (■) 9–16N.

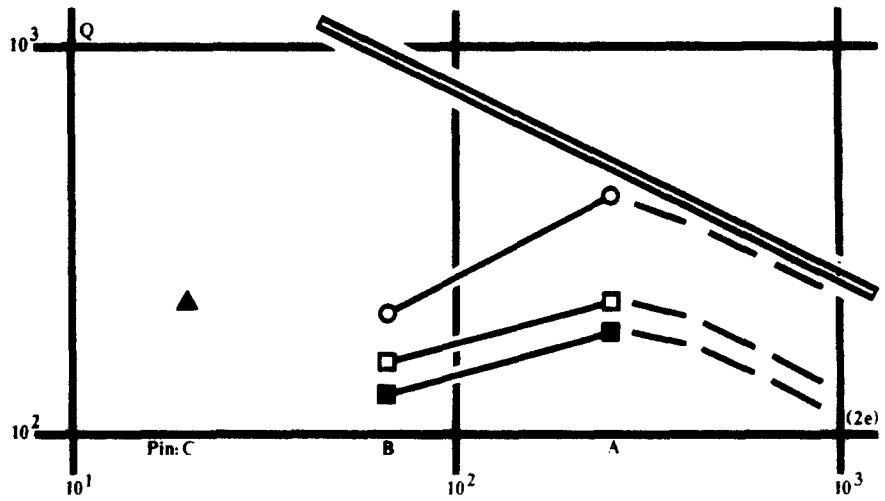

Fig. 9. Flypast severity term Q at onset of contact loss versus diametral clearance $2e$ for degreased bearing. Key: as for Fig. 8.

6. INTERPRETATION OF RESULTS

The behaviour actually observed in the reduced clearance tests suggests that the theoretical models omitted some significant factors. In the first place, profile imperfections such as taper, ovality, barrelling and more local irregularities become more significant as the clearance is reduced. Thus, contact actually takes place not on a narrow rectangular strip as supposed, but at one or more local "high spots". The high degree of contact compliance observed at low loads might then be explained as due to quasi-Hertzian deformation of these high spots, although the extent of the departure from the ideal prediction remains surprising. It seems probable that such irregularities of form are also the cause of the inconsistent displacement loci observed under low clearance conditions.

Secondly, the results seem to leave no doubt that the presence of the air film is a dominant factor at the lower end of the practically useful range of clearances. It is perhaps surprising that this has not been brought out in previously published experiments; conceivably the effects have been disguised by instrumentation and recording limitations.

The effect of friction must also be considered. Under the conditions of the test rig, this would be expected to increase the amount by which the point of contact lags the nominal force vector direction as the latter rapidly changes and thus to increase the tendency to contact loss in the passage phase. This expectation is supported by the observed re-

sults for pin A, where the threshold values using degreased surfaces are consistently lower than those using trace lubrication. It follows that the friction still present in the lubricated case is probably the major contributor to the discrepancy between the latter and the predicted values.†

This reasoning suggests a possible explanation of the flypast results with the tighter pins. The greatly increased retarding effect of the air film in these cases has an influence similar to that of friction, and therefore increases the tendency to loss of contact. This apparently outweighs the beneficial effect of reduced clearances predicted by the theory for an idealised case. For clearances greater than those tested, that factor is no longer relevant, so the behaviour is likely to follow the trend suggested by the broken line extrapolation in Figs. 8 and 9. Another implication is that the theory would be followed more closely for shorter bearings, in which the air escape paths are reduced.

7. CONCLUSION

This investigation produced some surprising, but consistent results. Contact compliance was found to be anomalously high at relatively low contact loads, possibly due to the effect of irregularities on highly conformal surfaces. While the dynamic behaviour of relatively slack bearings was in many respects as predicted, the reduced clearance tests revealed a quite different regime, in which the tendency to loss of contact was not reduced as predicted, but the ensuing impacts were reduced much more than expected due to the major influence of the air film. Thanks to the latter effect, it may be added, the failure to predict contact loss correctly in these cases is of less practical significance.

Although the test rig differs in some important respects from a proper linkage mechanism, the physical nature of the phenomena observed is such that their presence must also be felt in any ludodynamic turning joint of a comparable scale. The main practical implication of the new findings is to clarify the proper application of existing theories, in which the effects of the air film and of profile irregularities are neglected. These theories have been shown (here and elsewhere) to provide valuable information on the effects of modified joint load vector loci in slack bearings. It is now clear that they should not be applied to the comparison of slack bearings with tight bearings.

Acknowledgements—The author gratefully acknowledges the assistance of Dr. R. Godlewski in the design of the apparatus, and the advice and encouragement of Prof. L. Maunder, at the University of Newcastle upon Tyne; the support of the Science & Engineering Research Council (U.K.) during this investigation; and the cooperation of the Directors of NEI Reyrolle Ltd.

† At lower values of R_1^* this effect is apparently marked by the error arising from the stiffness of the actuator springs, noted in Section 2.

REFERENCES

1. R. S. Haines, *Mechanism and Machine Theory*, **15**, 361–370 (1980).
2. S. W. E. Earles and O. Kilicay, *Proc. Inst. Mech. Engrs*, **194**(25), 249–258 (1980).
3. H. Funabashi, K. Ogawa and M. Horie, *Bull. JSME*, **21**(161), 1652–1659 (1978).
4. H. Funabashi, K. Ogawa, M. Horie and H. Iida, *Bull. JSME*, **23**(177), 446–452 (1980).
5. B. M. Bahgat, M. O. M. Osman and T. S. Sankar, *J. Mech. Engng Sci.*, **21**(6), 429–437 (1979).
6. M. O. M. Osman, B. M. Bahgat and T. S. Sankar, ASME paper 80-WA/DSC-36 (1980).
7. R. S. Haines, *J. Mech. Engng Sci.*, **22**(5), 267 (1980).
8. R. S. Haines, Dynamic behaviour of linkage mechanisms, Ph.D. Thesis, University of Newcastle upon Tyne, England, 69–131 (1982).
9. O. Perera and W. Seering, ASME paper 82-DET-134 (1982).
10. M. T. Bengisu, D. Zuccaro and B. S. Thompson, ASME paper 82-DET-16 (1982).
11. R. J. Roark and W. C. Young, *Formulas for Stress and Strain, 5th Edition*, Table 33, Case 2, McGraw-Hill, Kogakusha, Tokyo (1975).
12. S. Dubowsky and F. Freudenstein, Trans. ASME, *J. Engng Ind.*, **93B**, 305–316 (1971).
13. K. P. Singh and B. Paul, cited in Trans. ASME, *J. Engng Ind.*, **97B**, 1168 (1975).
14. A. Scholes and E. M. Strover, *Int. J. Num. Methods in Engng*, **3**, 45–51 (1971).
15. V. A. Eshwar, *Int. J. Mech. Sci.*, **20**, 477–484 (1978).
16. S. W. E. Earles and C. L. S. Wu, Predicting the occurrence of contact loss and impact at a bearing from a zero-clearance analysis, *Proc. IV World Cong. IFToMM*, Newcastle upon Tyne, England, 1013–1018 (1975).
17. R. S. Haines, *J. Mech. Engng Sci.*, **22**(3), 129–136 (1980).
18. R. S. Haines, An experimental study of ludodynamics in a revolute joint, *Proc. VI World Cong. IFToMM*, New Delhi, India, 725–728 (1983).

APPENDIX 1

Alignment checks

A high accuracy of alignment was found to be necessary to obtain usefully repeatable results. This was achieved as follows—with the four displacement signals displayed in (X, Y) mode on two storage oscilloscopes and hand-force applied to the links, the pin/journal alignment is adjusted until the freedom of movement of the latter is roughly maximal on both axes, and then the suspension spring (g, Fig. 1) is adjusted until the journal is exerting little or no force on the pin. In this condition, gentle vertical motions of the journal (with the vertical link held against an adjustable stop) are used to check that the overall gains of the four channels are equal. Trajectories are then recorded on the screens as the journal is pushed around in circular fashion, first in very light ("point-") contact, then in firm ("line-") contact with the pin. By further adjustment of the pin/journal alignment, these trajectories are brought, as nearly as possible, coincident.

For the flypast tests, the loading balls must be correctly aligned. Initially, they are approximately centralised by eye. The axial position of each exciter is adjusted until its piston is working about its mid-travel position. Both exciters are opened to the gas line, whose regulated pressure is varied between (say) 3 and 20 bars. If this causes the two oscilloscope spots to move by different amounts, the exciters are exerting a moment on the journal, and one or

both balls must be moved slightly, parallel to the bearing axis, until the effect is eliminated. Similarly, if the pressure variation causes a change in the measured vertical component of pin load, the vertical alignment of the balls must be corrected.

APPENDIX 2

Calculations

All values are in dimensionally appropriate combinations of m, kg, sec units.

Drop tests. From Table 1, linear acceleration at test bearing = $(4 \times .110 \times 9.81/.051) \times .125 = 10.6$.

In eqn (1), let $R = 1000$, $L = .054$, $\nu_1 = .28$, $E_1 = 207 \times 10^9$, $\nu_2 = .3$, $E_2 = 69 \times 10^9$, $e = (250 \times 10^{-6}; 65 \times 10^{-6}; 20 \times 10^{-6})$, $D = .05$. Then $\delta_c = (1.07; 0.93; 0.81) \times 10^{-6}$. The total flexibility may be estimated by adding the mean contact compliance (δ_c/R) to the support flexibility (3.3×10^{-9}), that is $(4.2 \pm .2) \times 10^{-9}$ in each case. With effective mass $(.051/.125^2)$, this gives a natural frequency of ≈ 1350, that is half-period 0.37×10^{-3}. Mean of kinetic energy at approach and recoil is $\frac{1}{2}(.051/.125^2) V^2$. Peak elastic stored energy is $\frac{1}{2}P^2 \times 4.2 \times 10^9$ (for linearised spring). Equating the two, $P = 28 \times 10^3 V$.

Flypast tests. In the terminology of Ref. [17], (M_{uu}, M_{vv}) = (vertical, horizontal) total effective mass at bearing, that is $M_{uu} = .051/.125^2 = 3.25$, $M_{vv} = 4 + .015/.05^2 = 10$, and $M_{uv} = 0$. (Data from Table 1.) The dimensionless parametric groups H_2 and H_3 defined in [17] are therefore 0.51 and 0.0, respectively. Figure 5 of Ref. [17] gives predictions for $H_2 = 0.5$: for $H_3 = 0$, curve 1 (corresponding to the passage phase) predicts a contact-loss threshold at $H_1 = 0.17$. H_1 is defined as $R_u^*/(\dot{R}_v^{*2}\, e\, M_0)^{1/3}$ where $(R_u^*, \dot{R}^*)$ corresponds to $(|R_1^*|, |\dot{R}_H^*|)$ in the notation of this report and $M_0 \equiv \frac{1}{2}(M_{uu} + M_{vv}) = 6.63$: thus at the threshold,

$$(|\dot{R}_H^*| / |R_1^*|^{3/2}) = 5.5/\sqrt{e}.$$

APPENDIX 3

Methods of estimating $\dot{R}_H^*$

As the exciter master pistons pass through the mid portion of their travel, the force generated at the slave units changes at an approximately constant rate. Just before the journal starts to move, this applied force R_H^* only differs from the measured pin force R_H because of pin vibration (at a much higher frequency). Thus in cases where the latter is small, the underlying rate of change of R_H at this point in the cycle can be estimated directly from a trace of the signal and used as the value of $\dot{R}_H$. If the pin vibration is excessive, it can be momentarily reduced in the case of live readings by hand pressure on the journal so as to increase $|R_1^*|$.

In the case of tape-recorded signals an indirect method is used. For a given gas pressure, the waveform of $\dot{R}_H^*$ is to a first approximation constant as the frequency (eccentric shaft speed) is varied, except for the change in the time scale, that is, the value of $|\dot{R}_H^*|$ at mid-travel increases in inverse proportion to the period of the cycle. Accordingly, a value of $\dot{R}_H^*$ can be estimated as described above from taped records taken at the minimum shaft speed, and the change in cyclic period used to derive revised values for later points in the tape recording, as the shaft is accelerated.

APPENDIX 4

Method of constructing Figs. 8 and 9

For each test as described in Section 5, two values of $\dot{R}_H^*$ were noted, one at which the first signs of contact loss were judged to be apparent, the other at which contact loss was clearly established in both halves of the cycle. (In some cases these two values were identical). In eight tests with pin *A*, minimally oiled, at $R_1^* = 2$ Newtons, two additional values were noted, one at which the first signs of contact loss were apparent in both halves of the cycle and the other at which contact loss was clearly established in one half of the cycle (8). From each of the values noted, the term $(\log |\dot{R}_H^*| - (3/2) \log |R_1^*|$ was calculated.

For each combination of pins, lubrication condition and range of $|R_1^*|$, the average of the terms defined above, was calculated and shown by a single point on Fig. 8 or 9. The number of terms entering into each average is given in Table 2.

From each plotted value, a single estimate of the Wu and Earles index $(|\dot{R}_H^*|/|R_1^*|^{3/2})$ was computed using a representative value of R_1^*, namely 1, 2, 4, 8 and 16 Newtons for the five ranges shown in the figures. The range and logarithmic mean quoted in the text refer to these approximate summary values.

Table 2. Number of values averaged in construction of Figures 8 & 9

	Fig. 8					Fig. 9				
Curve	○	△	□	▲	■	○	△	□	▲	■
Pin A	4	34	12	8	8	2		2		2
Pin B	2	2	10		4	6		2		4
Pin C		2	2	4	2				2	

EINE EXPERIMENTELLE UNTERSUCHUNG DES DYNAMISCHEN VERHALTENS VON DREHGELENKEN MIT VERSCHIEDENEM GELENKSPIEL

Kurzfassung—Der Beitrag beschreibt einen Apparat (Bild 1) zur Untersuchung des Verhaltens eines spielbehafteten Drehgelenkes mit bekannten Gelenkspiel. Über drei Versuche mit diesem Apparat wird berichtet. Beim ersten Versuch wurde eine statische Belastung angewandt und der Ausschlag gemessen. Bei kleinen Belastungen war der gemessene Ausschlag überraschenderweise größer als der theoretische Wert. Beim zweiten Versuch wurde die Lagerbuchse ('b' im Bild 1) über den Spielraum fallengelassen. Im Falle des größten Gelenkspieles ($250 \cdot 10^{-6}$ m) bereiteten die Ergebnisse keine Überraschung (Bild 4a), aber im Falle des kleinsten Gelenkspieles ($20 \cdot 10^{-6}$ m) war die Bewegung viel langsamer (Bild 4c). Dies ist der hydrodynamischen Wirkung der Luft im Spielraum zuzuschreiben. Beim dritten Versuch wurde eine abwechselnde Horizontalbelastung zusammen mit einer nur kleinen ständigen Vertikalelastung aufgebracht. Dies ist mit den Bedingungen eines Lärm erzeugenden Koppelgetriebes zu vergleichen. Der Verlauf der Kontaktstelle an der Lagerbuchse und der Kraft am Bolzen wurden aufgenommen (Bilder 5, 6 und 7) und die Bedingungen für eine ununterbrochene Berührung der Gelenkelemente aufgezeichnet. Im Falle des größten Gelenkspieles (Bild 5) entsprachen die Ergebnisse teilweise der Theorie des Verfassers[17]. Im Falle der kleineren Gelenkspiele verminderten sich die Stöße und Schwingungen erheblich (Bilder 6 und 7), aber die Bedingungen für eine ununterbrochene Berührung entsprachen nicht mehr der Theorie. Diese Abweichung ist wahrscheinlich auch der Wirkung der Luft im Spielraum zuzuschreiben.